

Event-by-event fluctuation studies in the ALICE experiment

C. Zampolli^a for the ALICE Collaboration

Museo Storico della Fisica e Centro Studi e Ricerche Enrico Fermi (Rome) and INFN (Bologna), Italy

Received: 3 August 2006 /

Published online: 27 October 2006 – © Springer-Verlag / Società Italiana di Fisica 2006

Abstract. Event-by-event (E-by-E) fluctuations are considered to be one of the possible indications that a phase transition from ordinary hadronic matter to a plasma of quarks and gluons has occurred, as it is expected to happen in ultra-relativistic heavy-ion collisions. In this article, the results of a study concerning the observability of E-by-E fluctuations for the ALICE experiment at the LHC collider at CERN is presented. In particular, an estimate of the E-by-E statistical sensitivity in the measurement of the inverse slope parameter from the transverse momentum spectra of hadrons and of their particle ratios is discussed. The analysis relies on the excellent performance of ALICE in terms of particle identification.

1 Introduction

One of the main predictions of the lattice calculations of QCD (the theory of strong interactions) asserts that a phase transition from the ordinary hadronic matter to a deconfined state of quarks and gluons (the so-called quark-gluon plasma, QGP) should occur at very high temperature and energy density conditions. The nature of this phase transition (in other words the order of phase transition), and even whether this is more a crossover than a phase transition, and the existence of a (tri)critical end point are, however, topics still under discussion. Moreover, many parameters are involved, such as the value of the quark masses and that of the baryochemical potential μ_B .

The heavy-ion physics program of the large hadron collider (LHC) at CERN will concern Pb + Pb collisions at a centre-of-mass energy $\sqrt{s_{NN}} = 5.5$ TeV, allowing to investigate the unexplored regime of extreme energy densities ($\varepsilon = 15\text{--}40$ GeV/fm³), and high temperatures ($\mu_B \ll T$), where no sharp boundary is expected to show up between the hadronic matter and the QGP. The nature and the time evolution of the hot and dense system created in a heavy-ion collision will carry on the fingerprints of the QGP phase transition, which nonetheless may vary even dramatically from one event to the other. For this reason, an analysis on an event-by-event (E-by-E) basis will offer the opportunity to study the QCD phase transition and to get insights into the QGP.

E-by-E fluctuations may originate from different sources. Apart from the statistical fluctuations due to the geometrical properties of the collision [1–3], they may be related to the thermodynamics of the system (such as the temperature [4, 5]), to fluctuations of conserved quantities (such as the charge [6, 7]), to jets and minijets [8, 9], and

also to more exotic phenomena (such as disoriented chiral condensate (DCC) formation [10]).

ALICE (a large collider experiment) will be the experiment at the LHC dedicated to investigate the phase transition and the QGP in heavy-ion collisions. It will be able to perform event-by-event analyses thanks to the very high number of particles produced in each collision, and relying on its excellent particle identification capabilities. In this paper, the ALICE statistical sensitivity in measuring identified particle transverse momentum spectra and particle ratios (K/π , p/π) will be presented. In Sect. 2, the Monte Carlo event sample used for the analysis will be described. Section 3 will deal with the ALICE particle identification capabilities, fundamental as far as particle p_T spectra and particle ratios are concerned. Sections 4 and 5 will present the results of the analyses on the p_T spectra for identified pions, kaons and protons, and for K/π , p/π ratios, respectively. Finally, in the last section, the summary and the conclusions will be provided.

2 Monte Carlo event sample

The Monte Carlo event sample used for this analysis consists of 300 Pb + Pb central collisions at $\sqrt{s_{NN}} = 5.5$ TeV generated with the HIJING 1.36 Monte Carlo generator [11–14]. The impact parameter has been chosen to be in the range $0 < b < 5$ fm, corresponding to 10% of the total inelastic cross-section for Pb + Pb collisions at LHC ($\sigma_{\text{inel,Pb+Pb}}^{\text{tot}} = 8$ barn). The magnetic field has been set to $B = 0.5$ T. The GEANT3 package [15] has been used to track all the particles produced in the collision within the pseudorapidity range $|\eta| < 8$, and to simulate the detector signals and responses. Vertex reconstruction, particle

^a e-mail: Zampolli@bo.infn.it

Table 1. Mean number of charged (both negative and positive) primaries per event generated in the pseudorapidity range $-0.9 < \eta < 0.9$, with transverse momentum $0 < p_T < 4$ GeV/c. The values refer to the sample of 300 HIJING central Pb + Pb events used for the results presented in this article

Particle species	Number of primaries
π	7690
K	745
p	385

tracking, and particle identification have been performed as described in [16].

The mean number of generator-level primary charged (both negative and positive) particles¹ per event within the pseudorapidity range $-0.9 < \eta < 0.9$ and for $0 < p_T < 4$ GeV/c is reported in Table 1 for the three different particle species of interest in this analysis (i.e. pions, kaons and protons). The average charged particle multiplicity per unit rapidity per event is $dN_{\text{ch}}/dy \sim 4500$. The p_T value of 4 GeV/c corresponds to the upper limit of the transverse momentum range of interest for the event-by-event fluctuation analyses presented here (see Sects. 4 and 5), while the pseudorapidity interval $-0.9 < \eta < 0.9$ reflects the fiducial acceptance of the ALICE central detectors which have been used in this study.

3 Particle identification in ALICE

In the central rapidity region $-0.9 < \eta < 0.9$, inside the L3 magnet (which provides the experiment with a weak solenoidal magnetic field $B = 0.2\text{--}0.5$ T), ALICE will be endowed with subdetectors aimed at the tracking and the identification of the particles produced in the collisions. Going outwards from the centre of the experiment, the innermost detector is the ITS (inner tracking system), which is a silicon detector mainly aimed at the reconstruction of the primary and the secondary vertices. Then, next to the ITS, the ALICE main tracking device, the TPC (time projection chamber), will be installed, characterized by a momentum resolution $\sigma(p)/p < 2.5\%$ up to 10 GeV/c. Both the ITS and the TPC will be able to perform particle identification for charged hadrons via dE/dx measurements in the low momentum region ($p \lesssim 1$ GeV/c). After the TPC, the transition radiation detector (TRD), will concentrate mainly on the identification of high momentum electrons ($p > 1$ GeV/c) in the central region, playing also an important role in the ALICE particle tracking. At 3.7 m from the centre of the experiment, the time of flight (TOF) detector will be de-

voted to charged hadron identification in the intermediate momentum range ($0.5 \lesssim p \lesssim 4$ GeV/c). The central region will be also equipped with two small-area detectors: the HMPID (high momentum particle identification detector), a RICH detector which will carry out charged hadron identification in the high momentum range (up to $p \sim 3\text{--}5$ GeV/c), and the PHOS (photon spectrometer), a crystal calorimeter for the detection of electromagnetic particles. At large rapidity values, ALICE will be endowed with other detectors, namely the muon spectrometer, the zero degree calorimeter (ZDC), the photon multiplicity detector (PMD), the forward multiplicity detector (FMD) and the V0 and T0 detectors (for more details see [17]).

The event-by-event fluctuation studies reported in the following rely on the excellent capabilities of the ALICE experiment in terms of particle identification (PID). As a matter of fact, the ALICE experiment will be able to identify charged particles in a wide momentum range, from ~ 0.1 GeV/c up to a few GeV/c (and even more, up to a few tens of GeV/c, thanks to the TPC dE/dx measurements in the relativistic region [16]). This will be possible taking advantage of the particle identification capabilities of the various detectors, each playing a role in this sense in some narrower momentum range, complementary to the others. Besides, when some tracks are reconstructed simultaneously by different detectors, then a dedicated particle identification procedure can be applied, in order to combine all the available PID information.

For the analysis presented hereafter, the concern has been turned on the PID capabilities of the central tracking detectors ITS and TPC, and of the time of flight detector. The ITS, TPC and TOF enter the common Bayesian-approach framework adopted by every ALICE detector performing PID. This kind of approach allows to combine PID information of different nature, coming from different detectors, at the same time, with the advantage of being completely automatic. Moreover, it combines signals distributed according to quite different probability density functions. For more details on ALICE particle identification, see [16].

In particular, for the present study, the PID algorithm combines the signals from ITS, TPC and TOF making a logic “or” of them (ITS||TPC||TOF). This means that to each particle an identity is assigned provided that at least one of the three detectors has been able to perform particle identification on it. The main advantage of this choice is an increase in the number of useful tracks for the E-by-E analysis, even if at the expense of a higher contamination in the cases when only one PID signal is available.

Figure 1 shows the results of the combined PID algorithm when applied to the event sample, in terms of efficiency ε^{PID} and contamination C^{PID} defined as:

$$\varepsilon^{\text{PID}}(i) = \frac{N_{\text{id}}^{\text{t}}(i)}{N(i)}, \quad C^{\text{PID}}(i) = \frac{N_{\text{id}}^{\text{w}}(i)}{N_{\text{id}}^{\text{t}}(i) + N_{\text{id}}^{\text{w}}(i)}, \quad (1)$$

$N(i)$ being the number of particles of type i ($i = \pi, K, p$) reconstructed by the central tracking, $N_{\text{id}}^{\text{t}}(i)$ the number

¹ A particle is defined here as *primary* if its generated production vertex is less than 1 μm from the generated interaction vertex.

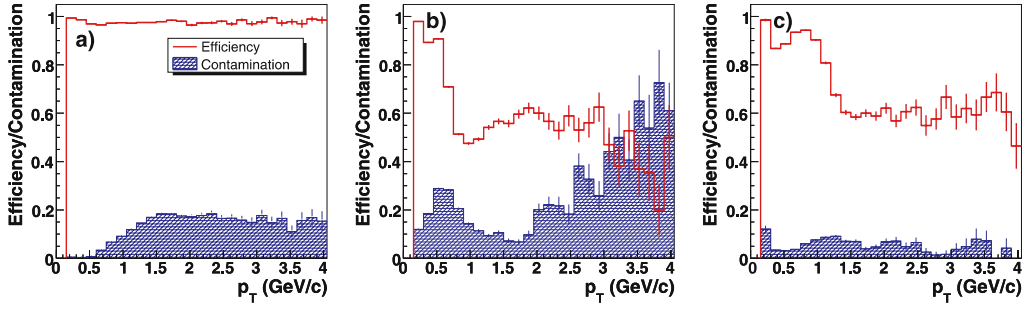


Fig. 1. Efficiency and contamination for the combined ITS||TPC||TOF particle identification procedure applied to 300 HLJING central events for the three particle species: pions **a**, kaons **b** and protons **c**

of i -particles correctly identified, and $N_{id}^w(i)$ the number of non- i -particles mis-identified as particles of type i . As one can see, as far as pions are concerned, the combined PID shows a contamination ranging from few percent to $\sim 20\%$, while the efficiency stays around 99%. The kaon efficiency varies between $\sim 70\%$ and $\sim 90\%$ in the low transverse momentum region ($0.15 < p_T < 0.75$ GeV/ c), and levels at a rather constant value $\varepsilon \sim 55\%$ up to $p_T < 3$ GeV/ c . At higher transverse momenta, a decrease in the kaon efficiency occurs, due to the fact that the kaon identification suffers from a reduction in the separation power of the TOF detector. In the case of protons, at low momenta ($p_T < 1.3$ GeV/ c) the efficiency ranges from 70 to 90%, while at intermediate and high p_T , it remains almost constant at a value of $\sim 60\%$. As far as contamination is concerned, for $p_T < 2$ GeV/ c the fraction of misidentified particles for all the three particle species ranges from few percent up to a maximum of $\sim 30\%$ for kaons. Still in the case of kaons, the substantial increase of the contamination for $p_T > 2$ GeV/ c is both due to a loss in the separation power of the TOF detector and to those particles identified by the TPC alone in the dE/dx relativistic rise region. Moreover, the peak at $p_T \sim 0.7$ GeV/ c corresponds to the overlap of the π and K bands in the dE/dx vs. p plane in the TPC.

For a summary, Table 2 quotes the efficiency and contamination from the combined PID technique, integrated over the corresponding transverse momentum ranges. The overall efficiency² for the three particle species is also quoted.

For the analysis presented herein, it is meaningful to derive the average number of particles of different species that can be identified per event by the combined PID technique. Table 3 quotes the number of pions, kaons and protons which are identified in a Pb + Pb central collision (the numbers are the mean values over the 300 events). As one can see, even in the case of kaons and protons, there is

Table 2. Efficiency, contamination, and overall efficiency for π , K , and p using the combined technique, integrated over the momentum range $0.15 < p_T < 4$, within the pseudorapidity range $-0.9 < \eta < 0.9$ (see text for more details)

	π	K	p
efficiency	98%	76%	86%
contamination	2%	22%	5%
overall efficiency	75%	39%	66%

Table 3. Average numbers of identified pions, kaons and protons per event. The distinction among the correctly (“true”) and the incorrectly (“wrong”) identification is reported

	π	K	p
N_{id}	5163	357	263
$N_{id,true}$	5058	277	250
$N_{id,wrong}$	105	80	13

a considerably high number of identified particles. This will make ALICE the first experiment able to perform event-by-event fluctuation analysis also for hadron species other than pions, with a highly efficient PID and over a wide momentum range.

4 Temperature fluctuations in ALICE

One of the main parameters in describing the system produced in heavy-ion collisions is temperature. Since the matter produced at the very early stages of the collision is thought to reach at least local thermodynamic equilibrium, trying to understand whether a unique temperature can trace the freeze-out, or if temperature fluctuations occur from event to event is of extreme interest.

Experimentally, temperature can be extracted from the slope parameters of p_T spectra. So, temperature fluctuations can be indirectly studied through the fluctuations in the inverse slope parameter derived from the transverse momentum spectra.

² The overall efficiency is defined as:

$$\varepsilon_{ov}(i) = \frac{N_{id}^t(i)}{N(i)_{prim}},$$

where $N(i)_{prim}$ is the number of generated primaries of type i . Since ε_{ov} is calculated with respect to the generated primaries, it takes into account different factors which affect the PID results, mainly the reconstruction efficiency, the effects of dead zones and of particle decays and interactions.

4.1 p_T spectra

Figure 2 shows the transverse momentum spectra separately for pions, kaons and protons obtained for the 300 HIJING central event sample described in Sect. 2. The distributions referred to as *identified* have been obtained with the combined particle identification procedure presented in Sect. 3. The labels *true* and *wrong* refer to correctly identified and mis-identified particles, respectively. From the shape of the spectra it is possible to infer that up to $p_T \sim 2$ GeV/c an exponential fit to the distributions would be a reasonable choice. For this reason, an event-by-event fitting procedure has been applied to the event sample for the three particle species in the transverse momentum range $0.25 < p_T < 2$ GeV/c, which sits below the high p_T region where the exponential form of the p_T spectra is no more expected [18–21], and which allows a good compromise between the efficiency and the contamination of the combined PID algorithm. For the transverse momentum spectra an exponential function of the form:

$$\frac{1}{2\pi p_T} \frac{d^2N}{dp_T dy} \propto \exp\left(-\frac{p_T}{T}\right), \quad (2)$$

has been used, where the inverse slope parameter T is the so-called “effective” temperature, related to the freeze-out temperature and to the mean transverse flow velocity [22, 23].

For each event, in order to recover the p_T spectra of the charged particles generated in the collision, the transverse momentum distributions of the identified hadrons have been corrected. Two correction factors have been applied. The first (ε) takes into account two “efficiency” contributions: (i) the limited geometrical acceptance of the detectors (ε^{acc}), implying that not all the generated particles undergo the PID procedure discussed in Sect. 3; (ii) the

particle identification efficiency (ε^{PID}), implying that not all the particles to which the PID is applied are correctly identified. The second correction factor (C) is instead due to the possible mis-identification of the charged hadrons (C^{PID}). From now on, the p_T distributions of the identified particles (“id”) corrected for both efficiency and contamination will be labelled as *reconstructed* (“R”) spectra. As a result, the relation:

$$\frac{d^2N}{dp_T dy}(\text{R}) = \frac{1}{\varepsilon}(1-C) \frac{d^2N}{dp_T dy}(\text{id}),$$

$$\varepsilon = \varepsilon^{\text{acc}} \varepsilon^{\text{PID}}, \quad C = C^{\text{PID}},$$

holds true. The efficiency and contamination factors have been calculated considering the whole event sample under study. Figure 3 shows the results of the fitting procedure for the three particle species for one of the simulated events. The generated transverse momentum spectra are drawn as well, as reference for the reconstructed spectra.

4.2 Fluctuations in the slope parameter

Figure 4 shows the distributions of the inverse slope parameters obtained for the 300 HIJING reference event sample, for pions, kaons, and protons. The results of the Gaussian fits performed over the distributions relative to the reconstructed hadron p_T spectra are shown together with those relative to the generated distributions. Table 4 summarizes the results. A good agreement can be observed among the mean inverse slope parameter values obtained considering the p_T distributions of the generated primaries, and the reconstructed ones. A small difference remains, probably due to the fitting procedure of the spectra which, in fact, are not rigorously exponential. On the other hand, the widths of the distributions of the inverse slope parameter for the generated p_T spectra are smaller than those

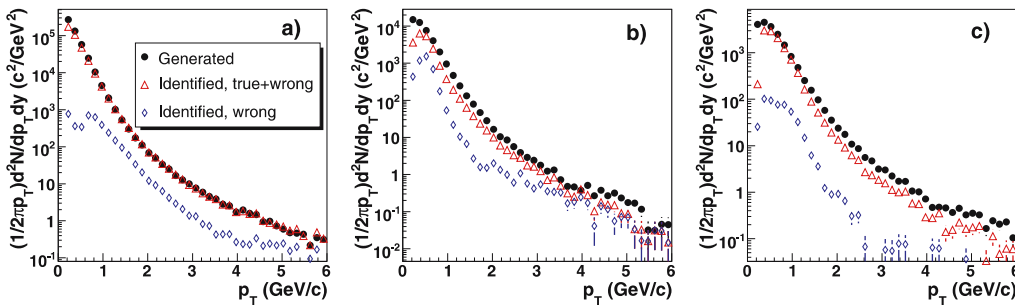


Fig. 2. Transverse momentum pion **a**, kaon **b** and proton **c** spectra for 300 HIJING central events

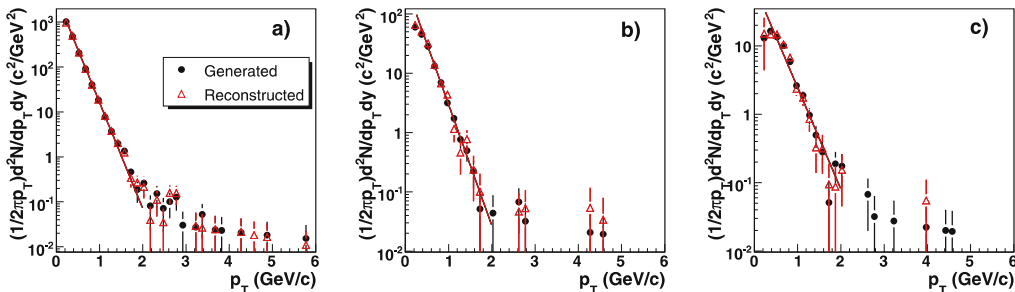


Fig. 3. Reconstructed (see text) p_T pion **a**, kaon **b** and proton **c** spectra for a single HIJING central event with the exponential fits of (2) superimposed. The generated spectra are drawn as well

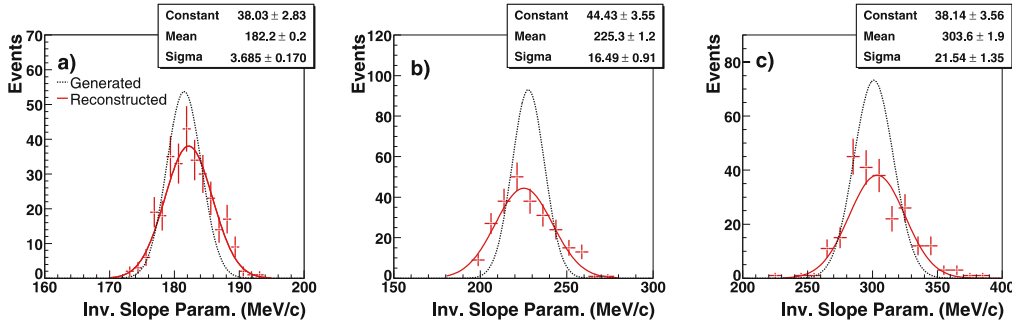


Fig. 4. Inverse slope parameter T distributions for reconstructed π **a**, K **b** and p **c** spectra. The Gaussian fits of the T distributions from reconstructed and generated spectra are superimposed. The fit parameters obtained for reconstructed hadron spectra are reported in the *top right panels*

Table 4. Mean inverse slope parameter values obtained from the Gaussian fits of the p_T distributions for generated (G) and reconstructed (R) π , K and p . In the last row, the σ of the Gaussian fits to the distributions relative to the reconstructed p_T spectra are quoted

	π	K	p
$\langle T \rangle$ (MeV/c) G	181.5 ± 0.2	227.8 ± 0.5	301.0 ± 0.9
$\langle T \rangle$ (MeV/c) R	182.2 ± 0.2	225.3 ± 1.2	303.6 ± 1.9
$\sigma(T)$ (MeV/c) R	3.7 ± 0.2	16.5 ± 0.9	21.5 ± 1.4

obtained from the reconstructed ones. This difference can be entirely understood in terms of the efficiency factors which relate the generated particle spectra to the reconstructed ones.

As one can see, the ALICE precision in terms of inverse slope parameter measurement is expected to be of the order of 2% for identified pions, and of 7% for both kaons and protons (see Table 4).

To be noted that an analysis concerning the distributions of the errors dT on the determination of the inverse slope parameter T , has shown that even if for each event the intrinsic value of dT is from a statistical origin, the mean value of the dT distributions is compatible with the width of the T distributions, as expected.

4.3 Determination of uncertainties

The uncertainty on the results from event-by-event studies is largely due to the limited number of particles which are taken into account. Apart from these statistical errors, there are other sources of uncertainties, such as the geometrical acceptance of the detectors, in-flight decays, the effects of multiple scattering, nuclear interactions with the materials in the detectors, and weak decays. Moreover, p_T cuts applied in the PID algorithm, or in the analysis, and the efficiency and contamination of the particle identification procedure can affect the observed particle spectra.

In order to estimate to what extent the systematic errors on the efficiency and contamination correction factors could affect the results, the correction factors have been varied by 10%. Notice that this choice is arbitrary (representing a reasonable guess for what is expected for the ALICE experiment), and that a more precise estimate of

the actual level of the systematic errors has still to be carried out in a dedicated study. This study has shown that no significant change in the mean values of the distributions occurs, either in the case of a 10% variation of the efficiency factor or in that of an analogous variation of the contamination factor. Similarly, the σ of the distributions, reflecting the precision with which the inverse slope parameter value can be known, are only slightly affected by systematic uncertainties.

5 Particle ratio fluctuations in ALICE

Besides the event-by-event inverse slope parameter T fluctuation analysis, the particle identification skills of the ALICE experiment will make it possible to study particle ratios, in particular K/π and p/π ratios. Figure 5 shows the result of the E-by-E particle ratio study performed on the 300 HIJING reference events. As in the case of T fluctuations, the particle identification has been performed with the combined PID algorithm (see Sect. 3), and the identified particle spectra have been corrected for efficiency and contamination as described in Sect. 4.1. The Gaussian fits to the reconstructed particle ratio distributions are superimposed, as well as the Gaussian fits to the generated ones. Table 5 quotes the results of the fits for the generated and reconstructed particles. As one can see, the results agree with each other within the errors.

The results show that the ALICE detector will be able to measure particle ratios with a statistical uncertainty of the order of $\sim 7\%$ and $\sim 9\%$ for K/π and p/π respectively.

6 Summary and conclusions

It has been shown that thanks to the very high particle yield per event and to an excellent PID capability, the ALICE experiment will be able to study fluctuations measuring the identified particle spectra for the three charged hadron species π , K and p , and the particle ratios K/π and p/π on an event-by-event basis. The statistical fluctuations affecting inverse slope parameter measurements are expected to be of the order of a few percent for all the three particle species, π , K , and p . As far as particle ratios K/π and p/π are concerned, the statistical fluctuations are again expected at the level of some percent. Any other con-

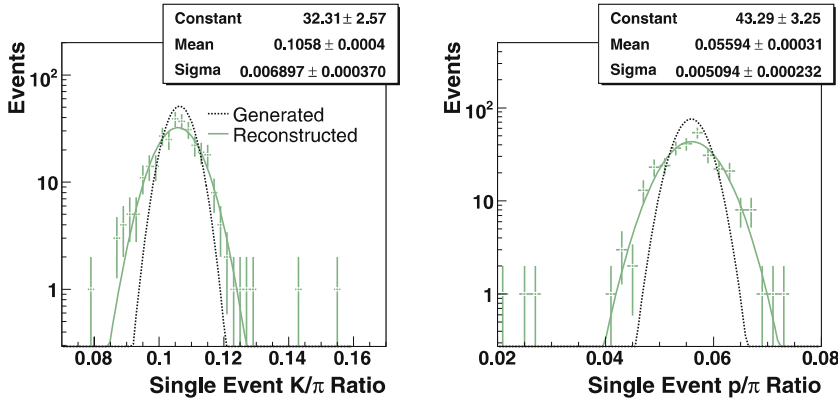


Fig. 5. K/π and p/π particle ratios for generated and reconstructed particles in the reference event sample. The parameters of the fit to the reconstructed particle ratios are reported in the *top right panels*

Table 5. Gaussian fit results for the distributions of the K/π and p/π particle ratios for generated (G) and reconstructed (R) particles

Particle ratio	K/π	p/π
Ratio G	0.1063 ± 0.0003	0.0558 ± 0.0002
Ratio R	0.1058 ± 0.0004	0.0559 ± 0.0003
σ (Ratio) R	0.0069 ± 0.0003	0.0051 ± 0.0002

tribution from dynamical fluctuations due to new physics may result in an increase of the observed values, or even in a distortion (non-Gaussian shapes) of the distribution.

A further comment is worth to be made concerning the dependence of the results presented herein on the assumed charged particle multiplicity per unit rapidity, dN_{ch}/dy . The Monte Carlo simulation with the HIJING generator used for the analysis presented so far provides $dN_{\text{ch}}/dy \sim 4500$ (central Pb+Pb collisions). The most recent studies have suggested lower values for dN_{ch}/dy , considering also the results from RHIC. The limit value of $dN_{\text{ch}}/dy \sim 1500\text{--}2000$ [25, 26] would imply a reduction by a factor $\sim 2\text{--}3$ in the observed number of charged particles, and, in turn, an increase by a factor $\sim \sqrt{2}\text{--}\sqrt{3}$ in the uncertainties on the E-by-E determination of the inverse slope parameters and particle ratios. Nonetheless, even in the case of a lower multiplicity, the number of identified π , K and p would still remain high enough to perform studies on an event-by-event basis, both in terms of inverse slope parameter and of particle ratio fluctuations.

On the other hand, a lower charged particle multiplicity would allow to obtain a better performance as far as track reconstruction and particle identification are concerned (see [16]), thus limiting the negative effect of the smaller statistics available. Moreover, if at $p_T \gtrsim 1.5$ GeV/ c the relative particle yields of π , K and p become comparable (as suggested from recent results at RHIC [24]), the PID performance would substantially improve, especially for kaons and protons. As a consequence, the uncertainties on inverse slope parameter and particle ratio measurements would be significantly reduced.

Finally, it also worth to remark that a more a precise and detailed E-by-E study will be possible thanks to the much larger number of events from the ALICE Physics

Data Challenge 2006, compared to the limited statistics (300 events) used for the results presented herein.

References

1. WA98 Collaboration, M.M. Aggarwal et al., Phys. Rev. C **65**, 054912 (2002)
2. M. Gaździcki, S. Mrówczyński, Z. Phys. C **54**, 127 (1992)
3. D.P. Mahapatra, B. Mohanty, S.C. Phatak, Int. J. Mod. Phys. A **17**, 675 (2002)
4. L. Stodolsky, Phys. Rev. Lett. **75**, 1044 (1995)
5. E.V. Shuryak, Phys. Lett. B **423**, 9 (1998)
6. J. Zaraneek, Phys. Rev. C **66**, 024905 (2002)
7. S. Mrówczyński, Phys. Rev. C **66**, 024904 (2002)
8. Q.-J. Liu, T.A. Trainor, Phys. Lett. B **567**, 184 (2003)
9. PHENIX Collaboration, M.J. Tannenbaum, et al., J. Phys. G **30**, S1367 (2004)
10. B. Mohanty, J. Serreau, Phys. Rep. **414**, 263 (2005)
11. X.N. Wang et al., Phys. Rev. D **44**, 3521 (1991)
12. X.N. Wang et al., Phys. Rev. Lett. **68**, 1480 (1992)
13. M. Gyulassy, X.N. Wang, Comput. Phys. Commun. **83**, 307 (1994)
14. OSCAR, Open Standard Code and Routines, <http://nt3.phys.columbia.edu/OSCAR>
15. R. Brun, F. Bruyant, A. Mc Pherson, P. Zancarini, Geant3 User Guide, CERN Data Handling Division DD/EE/84-1
16. ALICE Collaboration, ALICE: Physics Performance Report Volume II (2005) CERN/LHCC 2005-030, Eds. B. Alessandro et al. (ALICE Collaboration)
17. ALICE Collaboration, F. Carminati et al., J. Phys. G: Nucl. Part. Phys. **30**, 1517 (2004)
18. PHENIX Collaboration, K. Adcox et al., Phys. Rev. C **69**, 024904 (2004)
19. D. Teaney, J. Laurent, E.V. Shuryak, nucl-th/01110037 (2001)
20. D. Teaney, J. Laurent, E.V. Shuryak, Phys. Rev. Lett. **86**, 4783 (2001)
21. P.F. Kolb, R. Rapp, Phys. Rev. C **67**, 044903 (2003)
22. E. Schnedermann, J. Sollfrank, U. Heinz, Phys. Rev. C **48**, 2462 (1993)
23. T. Csörgo, B. Lorstad, Phys. Rev. C **54**, 1390 (1996)
24. PHENIX Collaboration, S.S. Adler et al., Phys. Rev. C **69**, 034909 (2004)
25. K.J. Eskola, P.V. Ruuskanen, S.S. Rasanen, K. Tuominen, Nucl. Phys. B **570**, 379 (2000)
26. M. Nardi, J. Phys. Conf. Ser. **5**, 148 (2005)